Bone strain and interfacial sliding analyses of platform switching and implant diameter on an immediately loaded implant: Experimental and 3D finite element analyses

Journal:	*Journal of Periodontology*
Manuscript ID:	JOP-09-0013.R1
Manuscript Type:	Original Article
Date Submitted by the Author:	
Complete List of Authors:	Hsu, Jui Ting; China Medical University, School of Dentistry Fuh, Lih Jyh; China Medical University, School of Dentistry Lin, Dan Jae; China Medical University, School of Oral Hygiene Shen, Yen Wen; China Medical University, School of Dentistry Huang, Heng Li; China Medical University, School of Dentistry
Key Words:	Implantology, Osseointegration, Treatment planning

Title: Bone strain and interfacial sliding analyses of platform switching and implant diameter on an immediately loaded implant: Experimental and 3D finite element analyses

Jui-Ting Hsu*/ Lih-Jyh Fuh* / Dan-Jae Lin/ Yen-Wen Shen*/ Heng-Li Huang*

* School of Dentistry, China Medical University, 91 Hsueh-Shih Road, Taichung 404, Taiwan.

School of Oral Hygiene, China Medical University, 91 Hsueh-Shih Road, Taichung 404, Taiwan.

*Corresponding Author: Heng-Li Huang. School of Dentistry, China Medical University, Taichung, Taiwan. Full Address: School of Dentistry, China Medical University, 91 Hsueh-Shih Road, 404 Taichung, Taiwan. Fax: 1-886-4-22014043 Phone: 1-886-4-22053366 ext. 2307. E-mail: hlhuang@mail.cmu.edu.tw

Financial support: This research was supported by Government Organization-National Science Council (NSC 97-2221-E-039-001) in Taiwan.

Word count in maintext (excluding abstract, references and figure legends): 2795

The number of figures and tables: 5 figures and one table

Running title: Platform switching on immediately loaded implant

Key finding from this study: Platform switching slightly reduces the bone strains in both delay-loaded and immediately loaded implants; in addition, micromotion at the bone-implant interface does not differ between implants with and without platform switching.

Abstract:

Objective: Both strain gauge analysis and finite element simulations were used to estimate the bone strain and micromovement at the bone–implant interface (BII) for platform switching and different diameters of a single immediately loaded mandibular implant. Methods: Four models were created including 5-mm-diameter implants assembled with abutments that were 5 or 4 mm in diameter on bonded (delay loading treatment) and contact (immediate loading treatment) BIIs; a model with an implant diameter of 3.75 mm was also analyzed. Vertical and lateral loads of 130 N were applied to all models. Results: During lateral loading, the strains were highly concentrated on one side of the mandible in both experimental and validation FE models. Bone strains were reduced by less than 10% when using platform switching compared to not using platform switching. However, increasing implant diameter decreased the surrounding bone strain significantly. The sliding and gap distances at the BII did not differ significantly among all the models considered. Conclusion: Bone strain is reduced more by increasing the diameter of an implant than by using platform switching in the immediately loaded implant. However, neither a wide implant nor platform switching reduces micromotion at the BII for enhancing implant stability.

Keywords: implantology, treatment planning, platform switching, immediate implant loading, biomechanics

Introduction

Immediate implant loading has been defined in a consensus conference meeting[1] as "a restoration placed in occlusion with the opposing dentition within 48 hours of implant placement". Due to the advantages of the immediate restoration of chewing functions and esthetics, the population of using immediately loaded implant as edentulous restoration treatment is increasing in clinics. Although studies have found that the survival rate of immediately loaded implants is acceptable[2,3], for single-tooth restoration immediately loaded implant is still considered to have a higher risk[4] and lower success rate[5]. These drawbacks might be due to increased micromovement at the bone–implant interface (BII)[6] , which leads the fibrous encapsulation around implant rather than full osseointegration[7]. This has resulted in a high reported variability (56–99%) in the survival of single immediately loaded implant[8]. In addition, some studies have indicated that the stress concentration is higher around the immediately loaded implant (contact BII)[9] than around the delay-loaded implant (osseointegrated BII)[10,11]. Because one of the causes of crestal bone loss is occlusal overloading[12], crestal bone loss might greatly influences on the esthetics and implant survival rate. These aspects make it worthwhile to investigate factors that could reduce the load burden on bone especially for single immediately loaded implants.

Platform switching refers to placing a smaller abutment on a larger-diameter implant to create a horizontal gap at the implant–abutment junction. According to Lazzara and Porter's study[13], radiography follow-up shows that platform switching reduces the loss of crestal bone height. They attributed this to the shifting inflammatory cell infiltrate away from crestal bone, because such infiltrate might appear within the gap of the implant–abutment junction. Recent studies have also investigated the biomechanical performance of platform switching[14,15]. Because platform switching changes the

traditional design of the abutment–implant connection, the stress/strain distributions from the abutment to the implant and from the implant to the bone might be influenced when occlusal loading occurred. However, for the immediately loaded implant the biomechanical effect of platform switching on stress/strain translation is still a controversial issue and remains to be investigated.

Increasing the implant diameter is an efficient way to enhance the contact between the bone and implant. The increased surface area might improve the holding support of the implant and influence stress transference[16] and the survival rate[17–18]. Although data from clinical and laboratory investigations of wide implants have been reported[20, 21], only a few studies have focused on the effects of immediate loading treatment on wide implants[11], especially in the mandible[22]. Implant diameter might also significantly influence immediate loading treatment, making it necessary to analyze the effects of implant diameter on the bone stress/strain and micromovement at the BII.

The purpose of this study was to determine the bone strain and micromovement at the BII for platform switching and for implants with different diameters using two testing methods: (1) experimental strain-gauge analysis with the rapid prototyping (RP) technique was applied to built the experimental models to measure the strain values of crestal cortical bone around the implant, and (2) finite element (FE) analysis with a nonlinear contact-interface simulation was used to create the three-dimensional (3D) computer models and evaluated the peak bone strains, bone strain distributions and the interfacial sliding distance at BII.

Materials and Methods

A series of computed tomography (CT) images of the posterior mandible of a dry human skull was obtained from the premolar to the first molar (Somatom Sensation 16,

Siemens Medical Solutions, Forchheim, Germany). The distance between adjacent CT images was 1 mm. From each CT image, material boundaries were delineated using our in-house imaging program "CTTOOLS", which employs various thresholds for the CT number and searches for maximum gradient values of the CT number. These gradient values were used to detect the boundary pixels between different materials. A depth-first search algorithm was then used to find the nearest boundary pixels and determine the coordinates of contour points for each material. The coordinated data were then fed to computer-aided design (CAD) software (SolidWorks 2007, Solidworks, Concord, MA, USA) to generate a 3D solid model of the posterior mandible.

Rapid prototyping and impression modeling

A resin model of the posterior mandible was constructed by using the RP technique and the impression procedures. The CAD model of the outer region (cortical bone) of posterior mandible was exported to a stereolithography file that was loaded into the 3D printer of an RP machine (ZPrinter 310plus, Z Corporation, Burlington, MA, USA) with zb56 binder and zCast 501 powder to create the prototypes of the bone model (Fig. 1a)[23]. The detailed geometry of the cortical shell was simulated using a lamination thickness of 0.004 in. However, because the RP model produced by the 3D printer is a powdered fabrication, drilling a hole and screwing an implant into the model can break the structure. Therefore, the cortical shell of the posterior mandible needed to be duplicated again using alginate impressions from RP model with temporary crown of acrylic resin. Then an epoxy resin was filled in to the core of the model of cortical shell to produce a replica of the trabecular bone (Fig. 1a). A self-tapping implant (ICE® self-tapping implant, 3i Implant Innovation, Palm Beach, FL, USA) (Fig. 1b) was then inserted into the resin model. The difference between the

models of immediately loaded implant and delay loaded implant was depended on the interface conditions of BII. In order to simulate the interface condition of an immediately loaded implant, the interface between implant and bone was contacted only. However, for models of delay-loaded implants, cyanoacrylate cement (CC-33A, Kyowa, Tokyo, Japan) was used to bind the surfaces of implant and bone model to simulate a bonded (osseointegration) interface. The cylindrical abutment (implant temporary hexed cylinder, 3i Implant Innovation) was then placed on the platform of the implant. Five models were prepared using this procedure: three immediately loaded implant models (a 3.75-mm-diameter implant with a 4-mm-diameter abutment, and 5-mm-diameter implants with 4- and 5-mm-diameter abutments) and two delay-loaded implant models (5-mm-diameter implants with 4- and 5-mm-diameter abutments).

The uniaxial compressive test was applied to quantify the material properties of the two resins. The elastic modulus was evaluated from the slope of the stress-versus-strain curve within the elastic region. In addition, Poisson's ratio was determined by measuring two strain values from biaxial strain gauges (KFG-10-120-D16-23, Kyowa) attached to the surfaces of cubic specimens of the two resins. These material properties (Table 1) were used in the simulations of FE models. The modeling procedures of the FE models are described below in the Finite element analysis section.

Mechanical testing

A self-developed jig was designed with an adjustable rotational screwing device so that both a vertical load and a 45-degree lingual oblique force could be performed in the experiments. Each loading mode involved applying a force of 130 N[24] to the cylindrical abutment using a universal testing machine (JSV-H1000, Japan

Instrumentation System, Nara, Japan) with a head speed of 1 mm/min. Rectangular rosette strain gauges (KFG-1-120-D17-11L3M3S, Kyowa) were attached to the buccal and lingual sides of the crestal cortical region around the implant (Fig. 3) using cyanoacrylate cement. Signals corresponding to the three independent strains ε_a, ε_b, and ε_c from the three gauges comprising the rosette strain gauge were sent to the data acquisition system (NI CompackDAQ, National Instruments, Austin, TX, USA) and analyzed by the associated software (LabVIEW SignalExpress, National Instruments). Each measurement was repeated three times. The maximum (ε_{max}) and minimum (ε_{min}) principal strains were obtained as follows:

$$\varepsilon_{max} = 1/2(\varepsilon_a+\varepsilon_c)+1/2\sqrt{[(\varepsilon_a-\varepsilon_c)^2+(2\varepsilon_b-\varepsilon_a-\varepsilon_a)^2]} \quad (1)$$

$$\varepsilon_{min} = 1/2(\varepsilon_a+\varepsilon_c)-1/2\sqrt{[(\varepsilon_a-\varepsilon_c)^2+(2\varepsilon_b-\varepsilon_a-\varepsilon_a)^2]} \quad (2)$$

The Student *t* test was applied to evaluate the difference of the peak values of maximum and minimum principal strains between the models with and without platform switching, wide diameter of implant, and immediate implant loading. All analyses were conducted in SAS version 9.1 (SAS Institute Inc., Cary, NC, USA).

Finite element analysis

The implants and abutments with two diameters (3.75 and 5mm) were created in the CAD software. After all the models of implant components and bone were combined using Boolean operations, the IGES format of the solid model was imported into ANSYS Workbench (Swanson Analysis, Huston, PA, USA) to generate the FE model (Fig. 2) using 10-node tetrahedral h-elements (ANSYS SOLID187 elements).

The material properties of the two resins, implant, and abutment are listed in Table 1[16]. For the models of delay-loaded implants, the nodes of the elements between the surface of the implant and bone was merged together as a bonded interface to simulate ideal osseointegration. For the models of immediately loaded implants, the contact

condition between the implant and bone was set with a frictional coefficient (μ) of 0.6. These values were then specified for the nonlinear surface-to-surface contact elements (ANSYS CONTA174 and TARGE170 elements) to simulate the sliding and sticking of frictional contact behavior at the BII. Two types of loading conditions were simulated: (1) a vertical force applied to the top surface of the abutment and (2) a lingual oblique force applied at 45 degrees to the long axis of the implant on the buccal site of the abutment (Fig. 2a). In both cases the applied force was 130 N. The mesial and distal surfaces of the mandibular bone were constrained to zero displacement in the *x*, *y*, and *z* directions as the boundary condition (Fig. 2a).

Results

Experimental testing

Except the models of

The difference in strain values between the models with and without platform switching, wide diameter of implant, and immediate implant loading was significant ($p > 0.05$) except the minimum principal (compressive) strain of the model of 5×13 mm_B_P versus that of 5×13 mm_B (B indicates bonded interface and P represents platform switching). The bone strains were higher in the models with a contact BII (3.75×13 mm_C, 5×13 mm_C_P, and 5×13 mm_C, where C indicates contact interface) than in those with a bonded BII (5×13 mm_B_P and 5×13 mm_B) (Fig. 3a and 3b). In addition, under lateral loading the compressive and tensile strains were highly concentrated on the lingual side, and the magnitude of the compressive strain was higher than that of the tensile strain. The difference in bone strains between the bonded BII implants with and without platform switching (5×13 mm_B_P versus 5×13 mm_B) was less than 5%. For the contacted BII, the peak compressive strains under vertical

and lateral loading were 7% and 8.3% lower, respectively, with platform switching than without platform switching (5×13 mm_C_P versus 5×13 mm_C). Compared to a 3.75-mm-diameter implant (3.75×13 mm_C), employing a 5-mm-diameter implant with a contact BII (5×13 mm_C) increased the bone strains by 90% under vertical loading, but decreased the bone strain by 48.3% under lateral loading.

Finite element analysis

For the models of 5-mm-diameter implants (Fig. 4a and 4b), compared to a bonded BII the contact BII increased the peak compressive and tensile strains under vertical loading by 28.5% and 30.8%, respectively, and the peak compressive strain under lateral loading by 54%. Under vertical loading, the bone strains did not differ between the implants with and without platform switching. Under lateral loading, the peak compressive strains for the bonded and contact BIIs were 9% and 5% lower, respectively, with platform switching than without platform switching. With a contact BII, the bone strains were 26.1% and 28.4% lower under vertical and lateral loading, respectively, in the 5-mm-diameter implant than in the 3.75-mm-diameter implant. Among the models with a contact BII, the sliding distance and gap distance (Fig. 4c) at the BII differed between the models with and without platform switching and between the models with and without using a wide-diameter implant by less than 3 μm under either vertical or lateral loading. The area with high bone strains was larger in models with a contact BII than in those with a bonded BII (Fig. 5). When using platform switching the strains were highly concentrated at the bottom of the abutment and at the top (the external hexagonal connection) of the implant (Fig. 5). However, the strain distribution of bone did not differ significantly between models with and without platform switching for both delay-loaded implants and immediately loaded implants (Fig. 5).

Discussion

A wider implant and platform switching are used to enhance the support provided by surrounding bone and prevent crestal bone loss. Although the biomechanical influences of platform switching and implant diameter have been discussed in several articles[14,15,25], most previous studies have only considered these two factors for delay-loaded treatment, in which the BII is osseointegrated (bonded). However, more dentists are using immediately loaded implants to restore single missing teeth, for which the biomechanical behavior of the interfacial contact at the BII on these two factors remains unknown. Therefore, this study used both experimental strain-gauge analysis and nonlinear FE contact simulation to investigate the effects of implant diameter and platform switching, which play different mechanical roles in influencing the bone surrounding an immediately loaded implant.

In the experimental tests, the strains were measured locally by strain gauges at selected locations. Even though the strain gauges were located close to the bone around the implant, they would be unable to measure the peak value of the bone strain when this occurs within the bone. However, in the FE analyses the peak values of the strain in bone were easily selected for the comparison; nevertheless, an FE analysis produces only an approximate rather than the exact solution. Therefore the combined use of experimental testing and FE analysis—as in this study—might facilitate the understanding of biomechanical mechanisms underlying the properties of single immediately loaded implants, and the effects of implant diameter and platform switching.

The strains were concentrated in the lingual side of cortical bone in both the experimental and FE models (Fig. 5b), especially under lateral loading. This indicates

that using an immediately loaded implant might induce a disproportionate strain distribution in bone. The delayed loading treatment produces a bonded BII (osseointegration), and the loads would then be dissipated evenly in both compressive and tension sites. However, for the immediately loaded implant the compressive and frictional forces can be transferred into the bone areas only where the implant surfaces contact. Therefore, forces mainly pass through contact sites, resulting in excessive strains, whereas strains are abnormally low at noncontact sites. These disproportionately low and high strains might result in a high risk of surrounding bone loss due to disuse atrophy or overloading resorption[26].

Many studies have indicated that using platform switching can reduce crestal bone loss[13, 27–31]. From the biomechanics viewpoint, a previous study[14] indicated that platform switching moved the stress concentration away from crestal bone. Nevertheless, that study only simulated the application of a vertical force at the edge of the abutment, and hence more quantitative evidence is needed to support this hypothesis. The present study analyzed both vertical and lateral loading modes in both immediately loaded and delay-loaded implants. Our results were similar to those of Schrotenboer et al. [15], in that platform switching reduced bone strains by less than 10%. In addition, even though platform switching changed the strain pattern at the connection between the implant and abutment, the strain distribution of crestal bone did not differ significantly between the models with and without platform switching (Fig. 5). Therefore, maintaining the cervical bone level platform switching—especially for the external hexagonal connection—did not provide obvious biomechanical advantage. The benefit of platform switching was also claimed by Lazzara et al.[13], with inflammatory cell infiltrate moving inwardly at the implant–abutment gap and away from crestal bone to prevent the bone loss. However, more scientific evidence is

needed to confirm this biological benefit.

The reduction in crestal bone strain was greater for the 5.0-mm-diameter implant than for the 3.75-mm-diameter implant. For the delay-loaded implant, increasing the implant diameter is known to increase the osseointegrated area at the BII, which would reduce the stress/strain around crestal bone during occlusal loading[16,25]. This might also reduce the risk of bone loss due to overloading[12]. The present study found that a wide implant provided biomechanical benefits not only for the delay-loaded implant but for the immediately loaded implant. The decrease in crestal bone stress induced by increasing the diameter of an immediately loaded implant has also been confirmed in the maxilla by Huang et al.[11]. Therefore, based on the biomechanics of view using a larger diameter implant is recommended for single implant placement in the immediate loading treatment.

The differences in sliding and in the gap distance at the BII were fairly small between models with and without platform switching and with different diameters. That shows that both factors did not enhance the implant stability. However, the review of Szmukler-Moncler et al.[32] indicated that the threshold for tolerable micromotion at the BII might be between 50 and 150 μm. In our models the resin used to form cortical bone (E=2979MPa, E represents Young's modulus) was 5 times softer than real cortical bone (E=15475MPa)[33], but the peak values of sliding and gap distances of the contact interfaces in immediately loaded implants were still lower than the threshold value (50 μm) when there was no gap at BIIs before applying a load. The micromotion threshold might differ with the implant surface type and design; nevertheless, based on a fine implant placement (such as a press-fit with no gap at the BII), the present study showed that a single immediately loaded implant can facilitate osseointegration.

Limitations of this study are the homogeneous, isotropic material properties of bone

model, as well as a static occlusal force used. In this study, the bone model was made from two resins. To the best of our knowledge, the real bone properties with anisotropic assumption may result in different stress/strain patterns; this requires further studies. Otherwise, although oblique load have been suggested to represent a realistic occlusal load[34], the chewing movement especially a dynamic loading simulation still needs to be considered in the further investigation.

Conclusion

Based on the results of experimental testing and FE analysis, the following conclusions can be drawn:

1. Bone strains are higher in an immediately loaded implant than in a delay-loaded implant.
2. Platform switching slightly reduces the strain in crestal bone. However, increasing the implant diameter decreases the bone strain in both delay-loaded and immediately loaded implants.
3. Micromotion at the BII does not differ between implants with standard and wide diameters, or between implants with and without platform switching.

Acknowledgement

This research was supported by Government Organization-National Science Council (NSC 97-2221-E-039-001) in Taiwan. All of the authors have no financial relationship to any private companies and organizations. We thank Dr.Chen-An Tsai, Ms.Kuan-Ting Chen and China Medical University Biostatistics Center for their help in statistical analysis

Reference

1. Cochran Dl, Morton D , Weber Hp. Consensus statements and recommended clinical procedures regarding loading protocols for endosseous dental implants. *Int J Oral Maxillofac Implants* 2004;19:109-113.
2. Attard NJ , Zarb GA. Immediate and early implant loading protocols: A literature review of clinical studies. *J Prosthet Dent* 2005;94:242-258.
3. Nkenke E, Fenner M. Indications for immediate loading of implants and implant success. *Clin Oral Implants Res* 2006;17:19-34.
4. Misch CE, Wang HL, Misch CM, Sharawy M, Lemons J , Judy KWM. Rationale for the Application of Immediate Load In Implant Dentistry: Part I. *Implant Dent* 2004;13:207-217.
5. Ioannidou E , Doufexi A. Does Loading Time Affect Implant Survival? A Meta-Analysis of 1,266 Implants. *J Periodontol* 2005;76:1252-1258.
6. Avila G, Galindo P, Rios H, Wang HL. Immediate Implant Loading: Current Status From Available Literature. *Implant Dent* 2007;16:235-245.
7. Gapski R, Wang HL, Mascarenhas P , Lang NP. Critical review of immediate implant loading. *Clin Oral Implants Res* 2003;14:515-527.
8. Wang HL, Ormianer Z, Palti A, Perel ML, Trisi P , Sammartino G. Consensus Conference on Immediate Loading: The Single Tooth and Partial Edentulous Areas. *Implant Dent* 2006;15:324-333.
9. Kao HC, Gung YW, Chung TF, Hsu ML. The influence of abutment angulation on micromotion level for immediately loaded dental implants: a 3-D finite element analysis. *Int J Oral Maxillofac Implants* 2008;23:623-630.
10. Huang HL, Fuh LJ, Hsu JT, Tu MG, Shen YW , Wu CL. Effects of implant surface roughness and stiffness of grafted bone on an immediately loaded maxillary implant: a 3D numerical analysis. *J Oral Rehabil* 2008;35:283-290.

11. Huang HL, Hsu JT, Fuh LJ, Tu MG, Ko CC , Shen YW. Bone stress and interfacial sliding analysis of implant designs on an immediately loaded maxillary implant: A non-linear finite element study. *J Dent* 2008;36:409-417.
12. Isidor F. Influence of forces on peri-implant bone. *Clin Oral Implants Res* 2006;17:8-18.
13. Lazzara RJ, Porter SS. Platform switching: a new concept in implant dentistry for controlling postrestorative crestal bone levels. *Int J Periodontics Restorative Dent* 2006;26:9-17.
14. Maeda Y, Miura J, Taki I, Sogo M. Biomechanical analysis on platform switching: is there any biomechanical rationale? *Clin Oral Implants Res* 2007;18:581-584.
15. Schrotenboer J, Tsao YP, Kinariwala V , Wang HL. Effect of Microthreads and Platform Switching on Crestal Bone Stress Levels: A Finite Element Analysis. *J Periodontol* 2008;79:1-9.
16. Huang HL, Huang JS, Ko CC, Hsu JT, Chang CH , Chen MYC. Effects of splinted prosthesis supported a wide implant or two implants: a three-dimensional finite element analysis. *Clin Oral Implants Res* 2005;16:466-472.
17. Winkler S, Morris HF, Ochi S. Implant Survival to 36 Months as Related to Length and Diameter. *Ann Periodontol* 2000;5:22-31.
18. Renouard F, Nisand D. Impact of implant length and diameter on survival rates. *Clin Oral Implants Res* 2006;17:35-51.
19. Brink J, Meraw SJ, Sarment DP. Influence of implant diameter on surrounding bone. *Clin Oral Implants Res* 2007;18:563-568.
20. Lee JH, Frias V, Lee KW, Wright RF. Effect of implant size and shape on implant success rates: A literature review. *J Prosthet Dent* 2005;94:377-381.
21. Davarpanah M, Martinez H, Kebir M, Etienne D , Tecucianu JF. Wide-diameter implants: new concepts. *Int J Periodontics Restorative Dent* 2001;21:149-159.

22. Degidi M, Piattelli A, Iezzi G, Carinci F. Wide-diameter implants: analysis of clinical outcome of 304 fixtures. *J Periodontol* 2007;78:52-58.

23. Liu Q, Leu MC, Schmitt SM. Rapid prototyping in dentistry: technology and application. *Int J Adv Manuf Tech* 2006;29:317-335.

24. Morneburg TR, Proschel PA. Measurement of masticatory forces and implant loads: a methodologic clinical study. *Int J Prosthodont* 2002;15:20-27.

25. Himmlova L, Dostalova T, Kacovsky A , Konvickova S. Influence of implant length and diameter on stress distribution: A finite element analysis. *J Prosthet Dent* 2004;91:20-25.

26. Frost H. Perspectives: bone's mechanical usage windows. *Bone Miner* 1992;19:257-271.

27. Hurzeler M, Fickl S, Zuhr O , Wachtel HC. Peri-Implant Bone Level Around Implants With Platform-Switched Abutments: Preliminary Data From a Prospective Study. *J Oral Maxillofac Surg* 2007;65:33-39.

28. Becker J, Ferrari D, Herten M, Kirsch A, Schaer A , Schwarz F. Influence of platform switching on crestal bone changes at non-submerged titanium implants: a histomorphometrical study in dogs. *J Clin Periodontol* 2007;34:1089-1096.

29. Guirado JLC, Yuguero MRS, Zamora GP, Barrio EM. Immediate Provisionalization on a New Implant Design for Esthetic Restoration and Preserving Crestal Bone. *Implant Dent* 2007;16:155-164.

30. Degidi M, Iezzi G, Scarano A , Piattelli A. Immediately loaded titanium implant with a tissue-stabilizing/maintaining design ('beyond platform switch') retrieved from man after 4 weeks: a histological and histomorphometrical evaluation. A case report. *Clin Oral Implants Res* 2008;19:276-282.

31. Cappiello M, Luongo R, Di Iorio D, Bugea C, Cocchetto R , Celletti R. Evaluation of peri-implant bone loss around platform-switched implants. *Int J Periodontics*

Restorative Dent 2008;28:347-355.

32. Szmukler-Moncler S, Salama H, Reingewirtz Y, Dubruille JH. Timing of loading and effect of micromotion on bone-dental implant interface: Review of experimental literature. *J Biomed Mater Res* 1998;43:192-203.
33. Van Oosterwyck H, Duyck J, Vander Sloten J, Van der Perre G, Naert I. Peri-implant bone tissue strains in cases of dehiscence: a finite element study. *Clin Oral Implants Res* 2002;13:327-333.
34. Geng JP, Tan KB, Liu GR. Application of finite element analysis in implant dentistry: a review of the literature. *J Prosthet Dent* 2001;85:585-598.

Figure Legends

Fig. 1. (a) Three-dimensional RP model of the cortical shell (lower object) used to mode resin into the model of cortical bone. The epoxy resin was poured into the core of the cortical bone to fabricate the model of trabecular bone (upper-right object). The rosette strain gauges were attached to the bone surface around the implant on both the buccal and lingual sides (upper-left object) (b). Self-tapping implants (D=5 mm and L=13 mm) with (left) and without (right) platform switching, which were inserted into the bone models.

Fig. 2. (a) Vertical loading and lateral loading modes were analyzed in FE models. The boundary condition involved fixing the inferior surface of the mandible (arrowheads). (c) Implants with platform switching of sizes 3.75 × 13 mm (upper), 5 × 13 mm (lower left), and 5 × 13 mm (lower right). The symbols of D, M, B, and L represent distal, mesial, buccal, and lingual directions.

Fig. 3. Peak strain values of the experimental models under vertical loading (a) and lateral loading (b). Max. P and Min. P represent the maximum and minimum principal strains, respectively. C, B, and P indicate contact interface, bonded interface, and platform switching.

Fig. 4. Peak maximum principal, minimum principal, and von-Mises strains of cortical bone in FE models under vertical loading (a) and lateral loading (b). Peak sliding distances and gap distances (c) at the BII in FE models under vertical and lateral loading.

Fig. 5. von-Mises strain distributions in the implant–abutment interface (left), implant body (middle), and surrounding bone (right) of delay-loaded implants (a) and immediately loaded implant (b) with and without platform switching under lateral loading. μS represents the microstrain. The column besides the figures indicated the different level of the strains value, and the area of red color represents high strain

values. The symbols of D, M, B, and L indicate distal, mesial, buccal, and lingual directions.

Table 1. Young's modulus and Poisson's ratio used in FE model.

Material	Young's modulus E (MPa)	Poisson's ratio v
Resin	2979	0.4
Epoxy resin	223	0.4
Titanium	110000	0.3

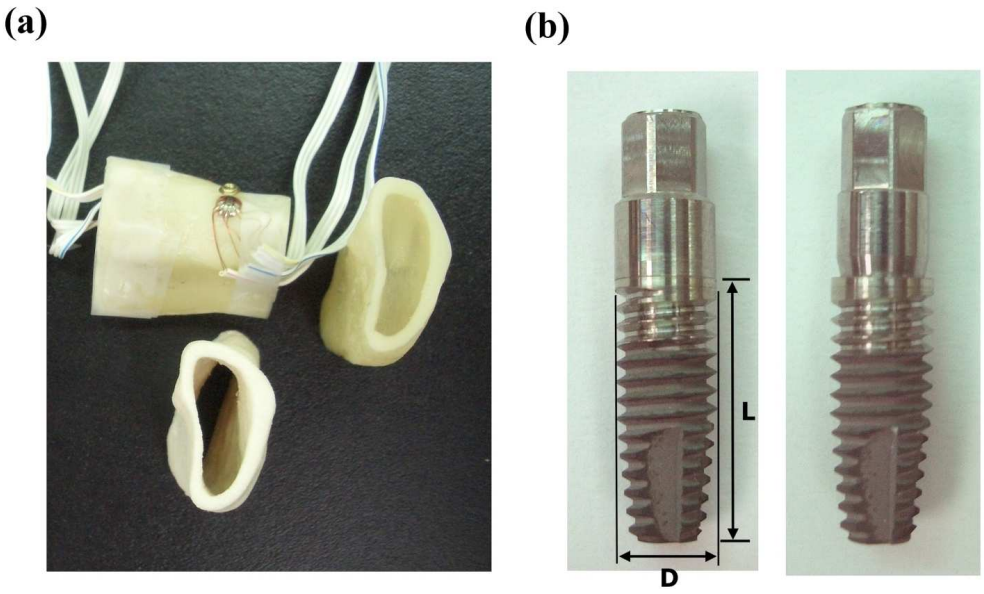

Fig. 1. (a) Three-dimensional RP model of the cortical shell (lower object) used to mode resin into the model of cortical bone. The epoxy resin was poured into the core of the cortical bone to fabricate the model of trabecular bone (upper-right object). The rosette strain gauges were attached to the bone surface around the implant on both the buccal and lingual sides (upper-left object) (b). Self-tapping implants (D=5 mm and L=13 mm) with (left) and without (right) platform switching, which were inserted into the bone models.
121x72mm (300 x 300 DPI)

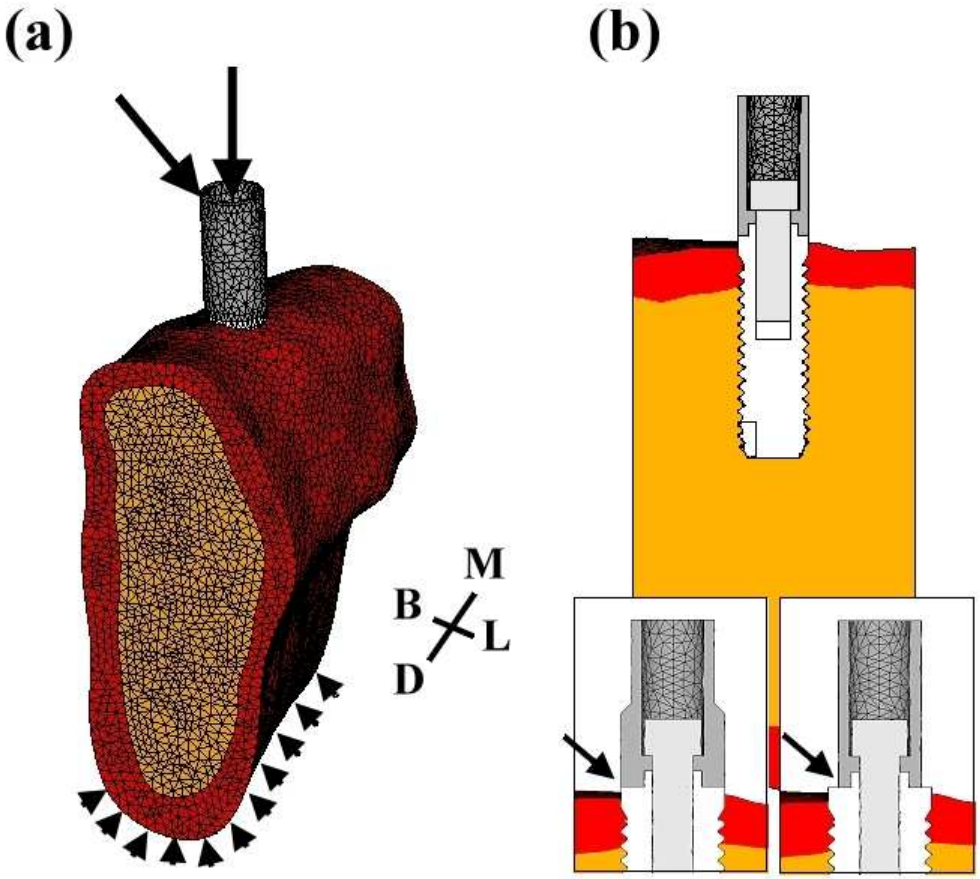

Fig. 2. (a) Vertical loading and lateral loading modes were analyzed in FE models. The boundary condition involved fixing the inferior surface of the mandible (arrowheads). (c) Implants with platform switching of sizes 3.75 ×13 mm (upper), 5×13 mm (lower left), and 5×13 mm (lower right). The symbols of D, M, B, and L represent distal, mesial, buccal, and lingual directions.

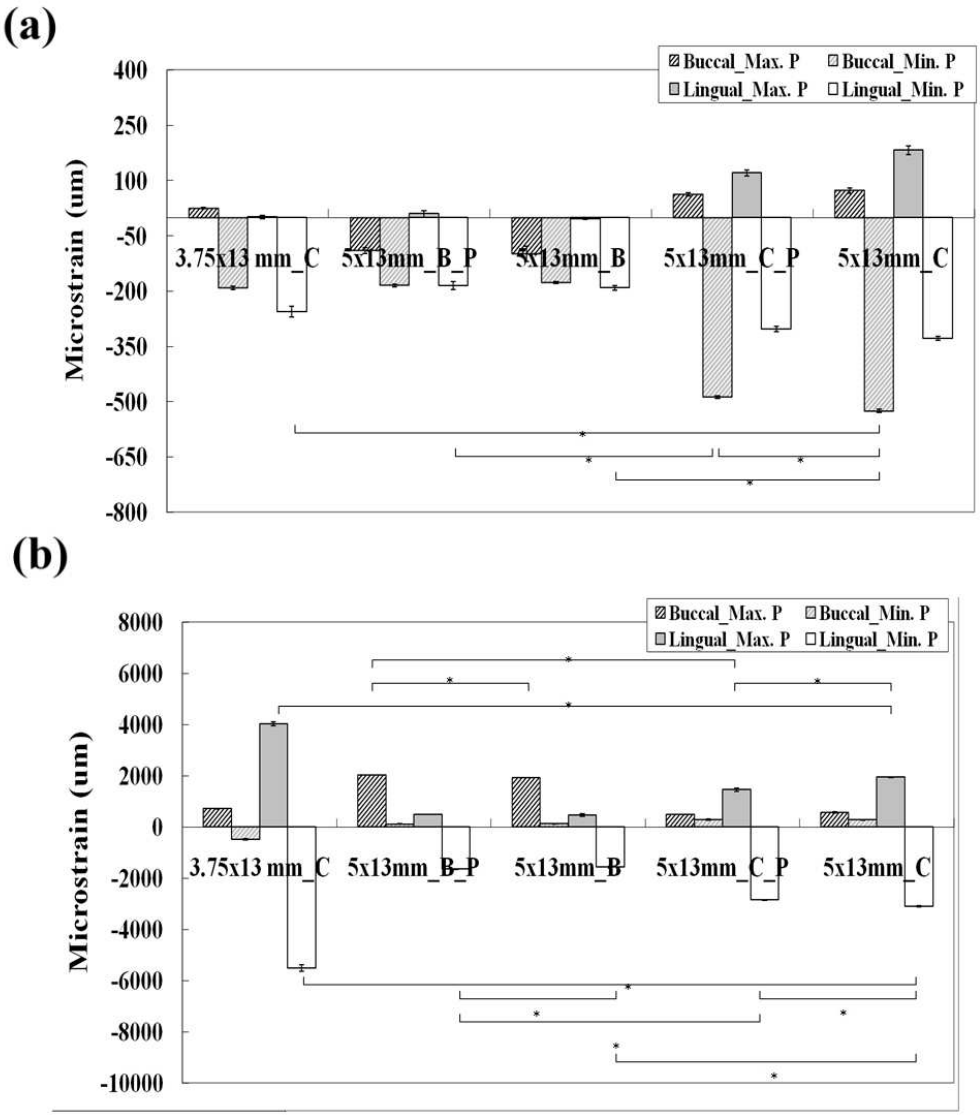

Fig. 3. Peak strain values of the experimental models under vertical loading (a) and lateral loading (b). Max. P and Min. P represent the maximum and minimum principal strains, respectively. C, B, and P indicate contact interface, bonded interface, and platform switching.

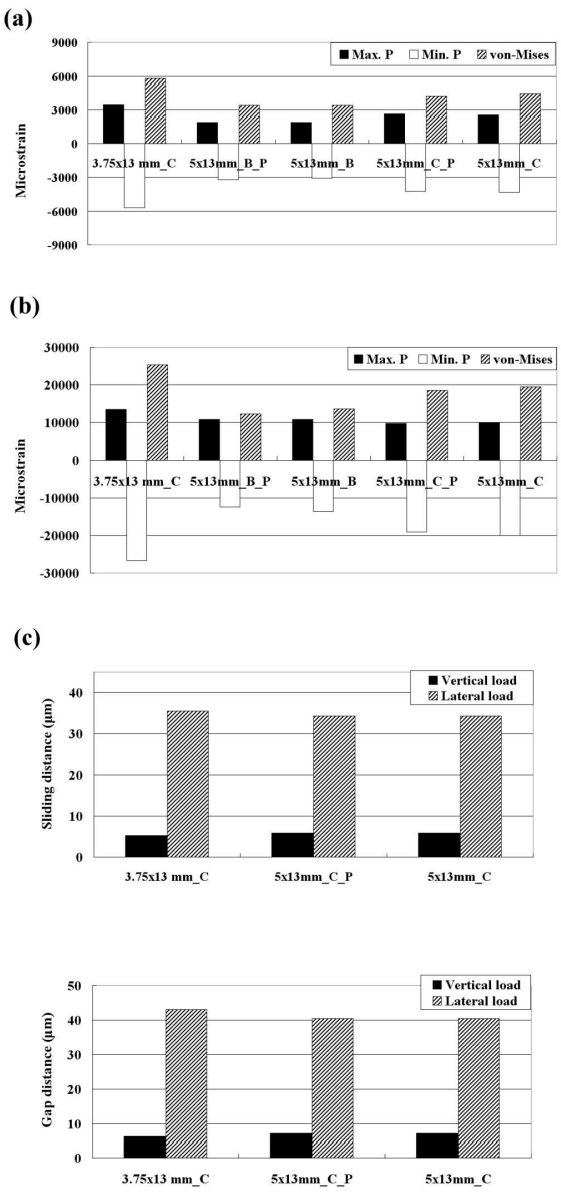

Fig. 4. Peak maximum principal, minimum principal, and von-Mises strains of cortical bone in FE models under vertical loading (a) and lateral loading (b). Peak sliding distances and gap distances (c) at the BII in FE models under vertical and lateral loading.
74x156mm (350 x 350 DPI)

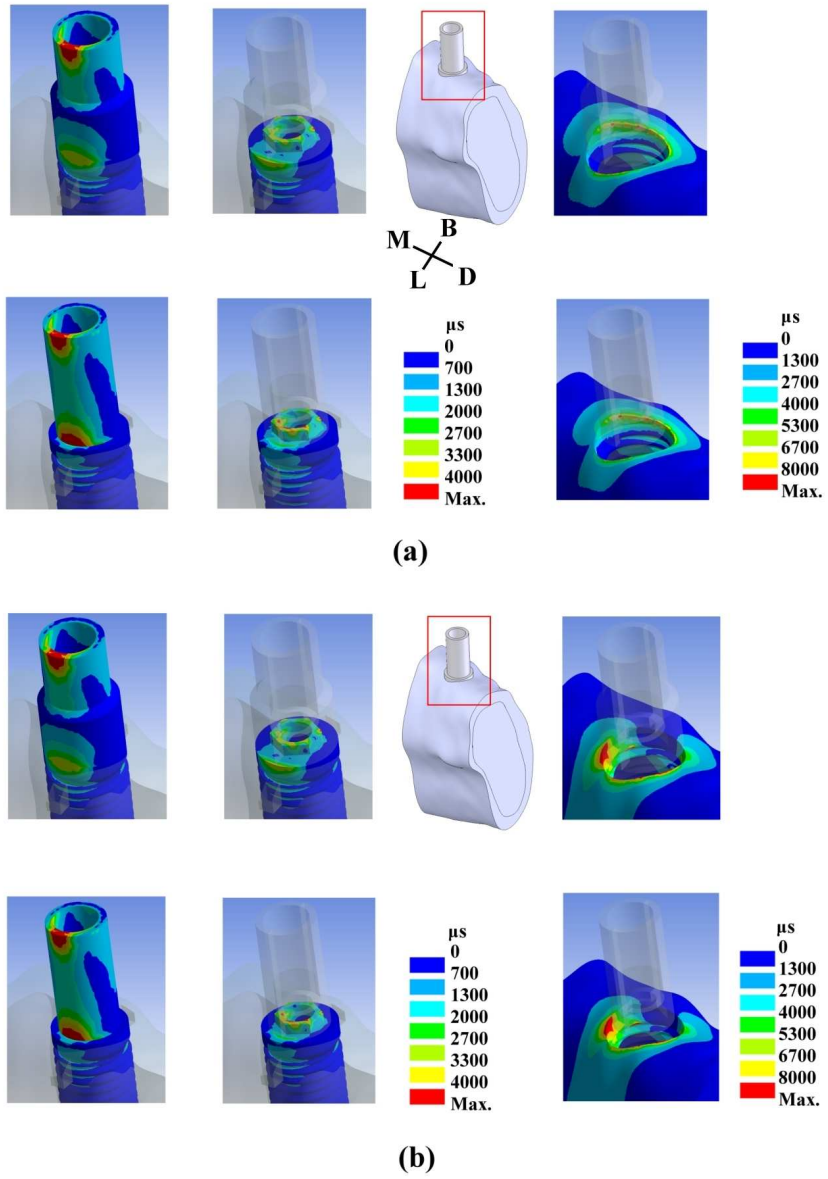

Fig. 5. von-Mises strain distributions in the implant–abutment interface (left), implant body (middle), and surrounding bone (right) of delay-loaded implants (a) and immediately loaded implant (b) with and without platform switching under lateral loading. μS represents the microstrain. The column besides the figures indicated the different level of the strains value, and the area of red color represents high strain values. The symbols of D, M, B, and L indicate distal, mesial, buccal, and lingual directions.